

Research Article

MICROBIOLOGY

Antibacterial activity of Silver Nanoparticles Biosynthesized by *Zingiber officinale* on Multi-Drug Resistant Bacteria

Mohamed M. Gharieb¹, Maged A. Elkemary², Azza M. Hassan³, Sally M. Gomaa^{1*}

¹Botany and Microbiology Department, Faculty of Science, Menoufia University, Shebin El-Kom, Egypt

²Institute of Nano science and Technology, Kafr El-Sheikh University, Kafr El-Sheikh, Egypt

³Medical Microbiology and Immunology Department, Tanta University, Tanta, Egypt

*Corresponding author: Sally M. Gomaa

email: sallymgomaa@gmail.com

Received: 20/2/2024

Accepted: 16/3/2024

KEY WORDS/

ABSTRACT

Zingiber
officinale,
AgNPs,
Biosynthesis,
MDR bacteria,
Antibacterial
activity

Current study dealt with the economical and environmentally friendly process of producing silver nanoparticles (AgNPs) through the use of an aqueous extract of ginger (*Zingiber officinale*) that is considered as ecofriendly and cheap method. The produced biosynthesized silver nanoparticles were characterized by UV-Vis spectroscopy, Transmission Electron Microscopy (TEM), X-ray diffraction (XRD), Fourier Transform Infra-Red spectroscopy (FTIR) and Zeta potential analysis. Then exhibited the antimicrobial activities of the biosynthesized silver nanoparticles against 30 clinically isolates of Multi Drug Resistant (MDR) bacteria which are *Staphylococcus aureus* (*S.aureus*), *Pseudomonas* spp., *Klebsiella* spp., *Escherichia coli* (*E.coli*) and *Proteus* spp. were carried out in Medical Microbiology and Immunology Department, Faculty of Medicine, Tanta University, after determined them by biochemical and antibiotic sensitivity tests. Then studied the effect of biosynthesized silver nanoparticles on the clinically isolated multi drug resistant bacteria by disc diffusion method. Additionally, Minimum Inhibitory Concentration (MIC) and Minimum Bactericidal Concentration (MBC) of biosynthesized AgNPs were estimated to be ranged from 31.25µg/ml to 250µg/ml and from 125µg/ml to 500µg/ml, respectively of tested MDR strains. Furthermore, the effect of AgNPs on the ultrastructure and morphology of the bacterial cells (*Proteus* spp. and *S.aureus*) showed the cell membrane rupture leading to the death of the cells compared with the untreated bacterial cells which detected by Transmission Electron Microscope (TEM) and Scanning Electron Microscope (SEM).

Introduction

Because of the present antibiotic treatments are ineffective against Multi Drug Resistant (MDR) bacteria, and the prevalence of antibiotic-resistant diseases is on the rise, posing a serious danger to public health (**Klevens *et al.*, 2007; Walker *et al.*, 2009**). Researchers are anticipating novel methods for the creation of alternative medications in order to combat microbes that are resistant to existing antibiotics. Misuse of antibiotics, in terms of application and dosage, is an additional contributing factor for the development of antibiotic resistance (**Nosanchuk *et al.*, 2014**).

Antimicrobial drugs are generally acting on the microbes by inhibiting a metabolic pathway such the inhibition of DNA/RNA synthesis or protein synthesis or disruption of the cell membrane (**Chethana *et al.*, 2013**) Microorganisms developed ability to overcome the drugs effect and can survive after exposure to these drugs and avoid getting killed (**He *et al.*, 2013**).

The study of nanostructures, particularly metallic nanoparticles (dimension between 1 and 100 nm in size), is the subject of the rapidly developing scientific discipline known as nanotechnology. Among many applications is its using as an antimicrobial agent. Silver nanoparticles

or AgNPs, have unique physical and chemical characteristics that make them ideal for a variety of applications, including drug delivery systems, wound healing, water purification, and sanitization (**Elechiguerra *et al.*, 2005; Krishnaraj *et al.*, 2010**). The significant threat of antibiotic resistance is mitigated by biosynthesized AgNPs, which are extensively employed as antibacterial agents against several MDR bacteria (**Hwang *et al.*, 2008**). The use of AgNPs in the development of a novel class of antimicrobial medicines has the potential to revolutionize the treatment of several bacterial infections (**Rai *et al.*, 2014**).

AgNPs may be synthesized using a variety of techniques, including chemical reduction, electrochemistry, photochemistry, and the green chemistry approach (**Kouvaris *et al.*, 2012**). The chemical route is the most prevalent method of AgNPs synthesis by reduction silver nitrate by using sodium borohydride (**Solomon *et al.*, 2007**). The absorption of borohydride is used in stabilizing the formed nanoparticles by providing particle with the surface charge. With the passage of time, the excess of sodium hydroxide increases the ionic strength then the nanoparticles will aggregate. The chemical methods

are wasting time and money (**Begum et al., 2009**). There has been growing recognition of biological approaches as a potential source for mining nanometals. These methods involve synthesizing nanoparticles utilizing plants, bacteria, fungus, algae, and yeasts. A simple biological approach to synthesizing AgNPs is an appealing area of study since it is both economical and environmentally beneficial, as it does not produce any harmful by-products. The scientists are recently found simpler ways of biological methods to prepare silver nanoparticles through biosynthesis methods using plant extract for reduction of silver nitrate and forming silver nanoparticles (**Bar et al., 2009; Song et al., 2009**). It also provides advantage of being save time, low cost and environment friendly. There is no need to use high pressure or temperature or any toxic chemicals (**Sondi et al., 2004**). This procedure might make use of a variety of fruit and plant extracts, including ginger, garlic, onion, and cinnamon. Traditional remedies sometimes use ginger, whose scientific name is *Zingiber officinale*, and which also adds a spicy flavor to our cuisine. Also, among its many respiratory uses, it alleviates nausea and asthma (**Rasool et al., 2022**). *Z. officinale* contains phytochemical substances that are

involved in metal reduction to metal nanoparticles.

The biochemical components of ginger such as zingerone, Oxalic acid, ascorbic acid, phenylpropanoids, saponins, flavonoids, terpenoids, phlobotannins, alkaloids, and glycosides play the role of reducing agents which convert silver ions into silver nanoparticles by passing through the stages of the silver nanoparticles formation as the chemical reaction including the steps of nucleation, condensation, surface reduction and stabilization (**Singh et al., 2011; El-Refai et al., 2018**) and also can Produce other types of nanoparticles such as AuNPs, CuNPs, and ZnONPs (**Raafat et al., 2021**).

In the past studies which showed that MDR microorganisms are present as contaminant on various medical equipment including ventilators and catheters. These infections, which are known as nosocomial infections *Pseudomonas aeruginosa*, can be rather dangerous (**Ansari et al., 2019**). It is more difficult to eradicate *Pseudomonas aeruginosa* due to its ability to develop both intrinsic and acquired resistance mechanisms that counteract the majority of antibiotic actions (**Salomoni et al., 2017**) and also *Staphylococcus aureus* which found naturally on human skin and in wounds, can cause bacteremia when it colonizes soft tissues of the skin

and spreads to other parts of the body (Ki and Rotstein, 2008). Healing failure and a rise in expected mortality are caused by these illnesses (Jain *et al.*, 2009) and when MDR *Staphylococcus aureus* was present, the healing failure will be worth. Therefore, this work set out to characterize AgNPs synthesized from ginger extracts, as well as to examine their antibacterial effectiveness against multidrug-resistant bacteria.

Materials and Methods

The plant and chemicals

The rhizomes of fresh ginger (*Z.officinale*) were bought at a nearby market. After washing three in sterile distilled water, the fresh ginger rhizome was chopped into small pieces and crushed to a weight of 20.0g. Then, 100 ml of sterilized distilled water was added, and the mixture was stirred continuously at 30°C for five hours. After passing the sample through a Whatmann No.1 filter paper, disinfecting the supernatant with a bacterial filter, and storing it in the fridge until needed, the procedure was complete. The dried ginger extract was made by drying 20.0g of fresh ginger in a hot air oven at 80°C for 6-8 hours, grinding it to a powder (1.3g), then adding it to 100 ml of sterilized distilled water while stirring continuously at 30 °C for 5 hours. We used Whatmann No. 1 filter paper was used to filter out the sample, and then the

supernatant was sterilized with a bacterial filter (0.22µm). Then it was stored in the fridge until use (Priyaa *et al.*, 2014; Dinda *et al.*, 2019; Şahin *et al.*, 2019; Hu *et al.*, 2022).

Biosynthesis of silver nanoparticles by ginger extract

Preparation of different samples of biosynthesized AgNPs solutions

Sample 1 (S1) was prepared by adding 10 milliliters of fresh ginger rhizome aqueous extract with 50 milliliters of 0.01M AgNO₃ (Sigma-Aldrich) was heated at 30°C for two hours using a magnetic stirrer heater. Sample 2 (S2) was prepared by the same methods of preparation of sample 1 but it was heated at 60°C. Sample 3 (S3) was prepared by adding 10 milliliters of the dried ginger rhizome aqueous extract was mixed with 50 milliliters of 0.01M AgNPs (Sigma-Aldrich) and heated for two hours using a magnetic stirrer heater 30°C and sample 4 (S4) was prepared with the same methods of preparation of sample 3 but it was heated at 60 °C. This study compared between the antibacterial activity of AgNPs that formed in the four prepared samples and detect the best effective one and compare between its antibacterial activity and its precursors (0.01M AgNO₃ and the ginger extract which help in the biosynthesis of it). The biosynthesized AgNPs in the four

samples were prepared in suitable amount and separated from the colloidal solution by highly speed centrifugation at 13000 rpm (Heraeus Multifuge X3R centrifuge, Thermo scientific, Germany), the precipitated biosynthesized AgNPs were washed with 95% ethanol solution and water (Yang *et al.*, 2016), respectively and then completely dispersed in the stock solutions with concentration 100µg/ml by using high powerful ultrasonic homogenizer (Cole-Parmer, USA) to use it in the following experiments.

The isolation and identification of MDR bacteria

This study was carried out on 70 samples collected from patients admitted to the surgical and burn units of Tanta University Hospital, the collected samples were passing through the following steps: All samples were collected under complete aseptic precautions. The exudate from the lesion was taken with a sterile swab, put into a sterile container and then was transported immediately to the lab of Medical Microbiology and Immunology Department, Faculty of Medicine, Tanta University for microbiological for analysis and processing. Each specimen was labeled with date and time of collection, patient name and number. The following media were used for the cultivation of all bacterial isolates:

nutrient agar (Oxoid, UK), blood agar (Oxoid, UK), MacConkey agar (Oxoid, UK), Muller-Hinton agar (Oxoid, UK), and Mannitol salt agar (Oxoid, UK). The purification has been done by agar streak plate technique, colonies of different shapes, color and showed separated growth on agar medium were picked up and re-streaked; after incubation, only growth of a single separate colony was picked up. All plates were incubated at 37°C for 24-48 hours. The isolates in the primary plates were identified by: Colony morphology: This included size, shape, surface, color of the colony and characteristic feature of the growth e.g. pigment production. Microscopic examination: Gram staining was performed for all the isolates to characterize and classify the organisms (Cheesbrough, 2006). The purified cultures were identified and confirmed after staining, investigating morphological characters, microscopic examination and biochemical tests. Biochemical tests were Oxidase test strips (Oxoid, UK), Hydrogen peroxide (3%)(Sigma-Aldrich) for catalase test, Peptone water (Oxoid, UK) and Kovac's reagent (Himedia, India) for Indole test. Citrated human plasma for coagulase test, Triple sugar iron (TSI) Agar slope (Oxoid, UK), Sugar fermentation tests (Oxoid, UK), Citrate utilization test (Oxoid, UK). Urease test (urea agar +

urea 40%) (Oxoid, UK) and soft agar for motility test (Oxoid, UK). The biochemical tests were conducted in accordance with Standard Clinical Laboratory protocols and the key to Bergey's manual by Krieg and Holt to identify the purified cultures. Staining and microscopic examination were also employed (Holt *et al.*, 1994; Cheesbrough, 2006). The modified Kirby Bauer disc diffusion technique was used to evaluate the antibiotic sensitivity of the isolates, following the recommendations set forth by the Clinical and Laboratory Standard Institute (CLSI, 2021), antibiotic discs were placed on Mueller Hinton agar plates. Among bacterial isolates; *Staphylococcus aureus*, *Klebsiella* spp., *Escherichia coli*, *Pseudomonas* spp. and *Proteus* spp. were determined as Multi Drug Resistant bacteria (MDR) by identification and antibiotic sensitivity testing (Bauer *et al.*, 1966).

Gram negative organisms were tested against the following

Colistin (10µg), Imipenem (10µg), Meropenem (10µg), Amikacin (30µg), Gentamicin (10µg), Tobramycin (10µg), Ceftazidime (30µg), Cefoxitin (30µg), Ceftriaxone (30µg), Cefepime (30 µg), Cefotaxime (30 µg), Aztreonam (30 µg), Amoxicillin/clavulanic acid (20/10 µg), Ampicillin- Sulbactam (10/10 µg),

Pipracillin/tazobactam (100/10 µg), Ciprofloxacin (5 µg), Ofloxacin (5 µg). Gram-positive organisms were tested against the following:

Penicillin G (10 units), Cefoxitin (30 µg), Erythromycin (15µg), Vancomycin (30µg), Doxycycline (5µg), Linezolid (30µg), Ciprofloxacin (5µg), Gentamicin (10µg), Tobramycin (10µg), Clindamycin (2µg), Ofloxacin (5 µg).

Distribution of microorganisms isolated from different clinical isolates

Only mono-microbial growth was detected in all isolated samples. Gram-negative organisms were the most common isolated microorganisms (72.58%, 51 isolates), *Pseudomonas* spp. had the highest percentage (24.28%, 17 isolates) followed by *Klebsiella* spp. (20%, 14 isolates), *E.coli* (15.71%, 11 isolates) and finally *Proteus* spp. (12.85%). Gram-positive organisms were isolated from 20% of samples (14 isolates) and *S. aureus* were the commonest with a percentage of (14.28%, 10 isolates), coagulase-negative *Staphylococci* (CoNS) (5.71%, 4 isolates) and *Candida* spp. (2.85%, 2 isolates) while (4.28%) 3 of samples showed no growth.

Antibiotic sensitivity testing of gram positive and gram negative bacteria

Out of all 65 culture confirmed bacterial isolates, 46.15% were MDR. 51 isolates of gram-negative bacteria,

49.02% of them were MDR, while out of 14 gram-positive bacteria, only 35.71% were MDR. 17 isolates of *Pseudomonas* spp. only 8 isolates (47.05%) were MDR. 14 isolates of *klebsiella* spp. only 8 isolates (57.14%) were MDR. 11 isolates of *E.coli* only 5 isolates (45.45%) were MDR. 9 isolates of *Proteus* spp. only 4 isolates (44.44%) were MDR. 10 isolates of *S.aureus*, only 5 isolates (50%) were MDR and no MDR was recorded for coagulase-negative *Staphylococci* (CoNS).

The percentage of the resistance of gram negative bacteria is from 37.5% to 100%. Gram negative bacteria had highest resistance to Ampicillin sulbactam and had the lowest resistance to Colistin. *Proteus* spp. had the highest resistance to 9 types of antibiotics (Amikacin, Gentamycin, Cefoxitin, Ceftriaxone, Cefepime, Aztreonam, Amoxicillin clavulanic, Ampicillin sulbactam and Ciprofloxacin). All MDR *E.coli* isolates showed resistance to tobramycin, ceftazidime, cefepime, amoxicillin-clavulanic, ampicillin-sulbactam, piperacillin-tazobactam, ciprofloxacin and ofloxacin. While (60% of MDR *E.coli* isolates) showed resistance to imipenem, Cefoxitin, Cefepime and colistin. All MDR *Klebsiella* spp. isolates were resistant to cefoxitin, ceftazidime, cefepime, cefotaxime, amoxicillin-clavulanic,

ampicillin-sulbactam and piperacillin-tazobactam. (50% of MDR *Klebsiella* spp. isolates) gentamycin, imipenem and only 37.5% of MDR *Klebsiella* spp. isolates were resistant to colistin. All MDR *Pseudomonas* spp. isolates showed resistance were resistant to gentamycin, tobramycin, ceftazidime, cefepime, piperacillin-tazobactam, ciprofloxacin and ofloxacin. The lowest resistance was to amikacin and colistin (50% of MDR *Pseudomonas* spp. isolates).

All MDR *S. aureus* had the highest resistance to 4 types of antibiotics (Penicillin G, Doxycycline, Ciprofloxacin and Ofloxacin), 80% of MDR *S. aureus* isolates were resistant to Cefoxitin and Gentamicin, 60% of MDR *S. aureus* isolates were resistant to Tobramycin and 40% of MDR *S. aureus* isolates were resistant to erythromycin. All MDR *S. aureus* isolates were sensitive to Vancomycin and Linezolid. Finally we get 30 clinically isolates Multi Drug Resistant (MDR) bacteria as the following gram negative bacteria:

8 isolates of MDR *Pseudomonas* spp., 8 isolates of MDR *Klebsiella* spp., 4 isolates of MDR *Proteus* spp. and 5 isolates of MDR *E.coli* and from gram positive bacteria: 5 isolates of MDR *S. aureus*.

Antibacterial activity of the biosynthesized AgNPs

The antibacterial activity of the produced AgNPs by *Z.officinale* (ginger) rhizome aqueous extract was carried out using Kirby Bauer disc diffusion method (Bauer *et al.*, 1966). By a sterile loop, 3-5 well isolated fresh colonies of similar appearance were picked up and emulsified in 3 ml of sterile saline. In a good light, the turbidity of the bacterial suspension was matched to the turbidity standard of 0.5 McFarland's against a sheet of paper. Bacterial colonies with an optical density (OD) of 0.10 at 625 nm and a bacterial suspension concentration of (1×10^8 CFU/ml, 0.5 McFarland's standard). Using a sterile cotton swab, a plate of Mueller Hinton agar was inoculated after dipping the swab in the inoculum suspension, rotating it firmly against the inside of the tube to remove excess fluid and evenly streaking it over the entire agar surface. After incubating at 37°C for 24 hours, the four biosynthesized AgNPs samples, with concentration 100µg/ml were evenly distributed onto 6-mm filter paper discs, which were subsequently inoculated an agar plate. The zone of growth inhibition was then quantified (mm). The most effective AgNPs sample on MDR bacterial isolates was chosen to be compared with its precursors (0.01M

AgNO₃ and the aqueous ginger extract that helped in the biosynthesis of it).

Determination of Minimum Inhibitory Concentration (MIC) and Minimum Bactericidal Concentration (MBC)

The Clinical and Laboratory Standards Institute (CLSI, 2012) technique was used to determine the MIC and MBC of the biosynthesized AgNPs. The MIC test was conducted on Muller Hinton Agar (MHA) plates from Oxoid, UK, whereas the MBC test was carried out on 96-well round bottom microtiter plates using conventional broth micro dilution procedures. To conduct the minimum inhibitory concentration (MIC) test, bacterial inoculums were produced in Muller Hinton Broth (MHB) medium (Oxoid, UK) at a concentration of 1×10^8 CFU/mL suspension was matched to the turbidity standard of 0.5 McFarland's standard. In order to determine the minimum inhibitory concentration (MIC) values of the biosynthesized AgNPs, a stock solution of the compound was diluted with sterile distilled water twice in a sequential fashion, starting with a concentration of 500µg/mL. The biosynthesized AgNPs had concentrations of 500µg/ml, 250µg/ml, 125µg/ml, 62.50µg/ml, 31.25µg/ml, 15.625 µg/ml, and 7.8125µg/ml. The microtiter plates were placed in an incubator set at 37°C for 24

hours after being sealed by the cover of microtiter plate to avoid evaporation. Using an ELISA microtiter plate reader (Stat Fax 2100 Micro plate Reader, Awareness Technology, Inc., USA), we monitored absorbance at 600 nm and measure the optical density (OD) for each well before and after the incubation for each well before and after incubation to determine the minimum inhibitory concentration (MIC) of the biosynthesized AgNPs. MIC was found to prevent observable bacterial growth to be detected by the micro plate reader (Erjaee *et al.*, 2017).

The minimum bactericidal concentration (MBC) of an antibacterial agent was defined as the concentration at which all bacteria were eradicated. 100 μ L of the suspension from each well of the microtiter plates was added to the MHA plate in order to analyze the MBC test. We incubated the plates at 37°C for 24 hours. We chose the MBC value since it was the lowest concentration on the MHA plate that did not produce any discernible growth. Triplicates of each experiment were carried out (El-Shennawy *et al.*, 2020).

Examination of the Bacterial Cells by SEM and TEM

Cells of the selected *Proteus* spp. (*Proteus* 2) and *S. aureus* (*S. aureus* 1) isolates were analyzed by TEM and SEM after treatment with AgNPs

combination for 12h and were compared to untreated cells (control). The minimum inhibitory concentration (MIC) of 250 μ g/ml of AgNPs was used to determine the concentrations utilized in this investigation. A bacterial inoculum of 1×10^8 CFU/ml was used in all of the cultures (Khalil *et al.*, 2021).

The influence of AgNPs on the morphology and ultrastructure of bacterial cells

Scanning Electron Microscope (SEM) (JSM-5300, Jeol, Japan) operated between 15 and 20 KeV which was used to observe the morphological changes of MRD bacteria (*S. aureus* and *Proteus* spp.) treated with biosynthesized AgNPs. To fix the bacteria, we submerged them in 4F1G (Fixative, phosphate buffer solution) with a pH of 7.4 and incubated them at 4°C for three hours. This was followed by two hours of post-fixation in the same buffer containing 2% OsO₄ at 4°C. At 4°C, the samples were dehydrated using ethanol at varying concentrations after being rinsed in the buffer. In a sputter coating facility (JFC-1100 E), the samples were dried using a critical point approach, mounted on an Al-stub using carbon paste, and coated with gold up to a 400 Å thickness. Prior to embedding in resin, samples underwent fixation and dehydration procedures. Following this, they were put through a graded sequence

of acetone for Transmission Electron Microscopy (TEM). We used a Transmission Electron Microscopy (JSM-1400-Plus, JeoL, Japan) to look at the prepared blocks after we sectioned them, dyed them with uranyl acetate and lead citrate, and mounted them on a copper grid (Tahmasebi *et al.*, 2015).

Characterizations of the biosynthesized silver nanoparticles AgNPs

The biosynthesized silver nanoparticles were characterized via Ultraviolet-Visible spectroscopy (UV-2450 Shimadzu, Japan). Where, the absorbance was measured at (200-800 nm) spectral range. The charge of the nanoparticles was measured five times using a Brookhaven Zeta Potential analyzer (Brookhaven instruments corporation, USA), by adding 1 mg of biosynthesized AgNPs to 3ml of distilled water and dispersed homogenously in it then letting it sit at room temperature (Ibrahim *et al.*, 2016).

The plant extract was analyzed using Fourier transform infrared spectra (FTIR-6800, Jasco, Japan) to determine which functional groups may have reduced the silver ions and capped the AgNPs that were formed. For FTIR spectroscopic examination at room temperature along the 4000 - 500 cm^{-1} spectrum region, a tiny disc was formed by mixing the freeze-dried aqueous

extract of *Z.officinale* (ginger) with potassium bromide.

A revolving anode running at 35 kV and 35 mA with a copper target was used to conduct XRD (X-Ray diffraction) investigation, with peaks occurring between 10° and 80° in 2°. The instrument used was the X-ray diffractometer (GNR-APD-2000 Pro, Italy).

The shape and size of the biosynthesized AgNPs were detected using transmission electron microscopy (TEM) (JSM-1400-Plus-JeoL, Japan) of the generated particles. We use a transmission electron microscope to examine the sample after ultrasonicated a solution containing biosynthesized silver nanoparticles and putting it onto a copper grid. We then wait for the grid to dry (Yue *et al.*, 2004).

Statistical analysis

To facilitate the data analysis, statistically analysed using SPSS software statistical computer package for Windows, version 21 (IBM Corp., Armonk, N.Y., USA). For normally distributed data, values were expressed as mean, standard deviation (SD). Student t test (T test) was used to compare 2 independent groups. P value (≤ 0.05) was adopted as the level of significance, P values < 0.001 were considered highly significant, while P

values > 0.05 were considered statistically not significant.

Results

Determination the effect of biosynthesized AgNPs on clinical MDR bacterial isolates

Table (1) Shows that the sample no.4 (S4) displayed the highest effect on MRD bacterial isolates *Klebsiella* spp, *Pseudomonas* spp., *E.coli*, *Proteus* spp. and *S. aureus*) with zone of inhibitions

Table (1): Zone of inhibition (mm) as an effect of four biosynthesized AgNPs samples against different MDR bacteria *Klebsiella* spp., *Pseudomonas* spp. *E.coli*, *Proteus* spp. and *S.aureus*. The data are the mean of 3 replicates \pm SD.

Bacteria	Inhibition zones diameters (mm)			
	AgNPs (S1)	AgNPs (S2)	AgNPs (S3)	AgNPs (S4)
<i>Klebsiella</i> spp.	9.60 \pm 0.57	10.60 \pm 0.57	10.90 \pm 0.57	12.50 \pm 0.57
<i>Pseudomonas</i> spp.	9.40 \pm 0.63	11.60 \pm 0.57	11.0 \pm 0.63	12.80 \pm 0.78
<i>E. coli</i>	9.30 \pm 0.57	11.20 \pm 0.66	11.40 \pm 0.74	12.30 \pm 0.57
<i>Proteus</i> spp.	9.50 \pm 0.57	10.80 \pm 0.57	10.80 \pm 0.78	11.60 \pm 0.57
<i>S. aureus</i>	9.70 \pm 0.57	11.70 \pm 0.74	11.70 \pm 0.66	12.50 \pm 0.57

Table (2): Zone of inhibition (mm) as an effect of AgNPs in (S4), 0.01M AgNO₃ and dried ginger extract against different MDR bacteria *Klebsiella* spp., *Pseudomonas* spp., *E.coli*, *Proteus* spp. and *S. aureus*. The data are the mean of 3 replicates \pm SD

Bacteria	Inhibition zones diameters (mm)		
	AgNPs (S4)	AgNO ₃ (0.01M)	Dried ginger aqueous extract (1.3g in 100 ml of sterilized distilled water)
<i>Klebsiella. spp</i>	12.50 \pm 0.57	9.30 \pm 0.78	6.0 \pm 0.0
<i>Pseudomonas spp</i>	12.80 \pm 0.78	9.10 \pm 0.71	6.0 \pm 0.0
<i>E. coli</i>	12.30 \pm 0.57	9.0 \pm 0.50	6.0 \pm 0.0
<i>Proteus spp</i>	11.60 \pm 0.57	9.40 \pm 0.50	6.0 \pm 0.0
<i>S. aureus</i>	12.50 \pm 0.57	8.80 \pm 0.50	6.0 \pm 0.0

Susceptibility of bacterial isolates to biosynthesized AgNPs (MIC, MBC and tolerance level values)

Antimicrobial activity of biosynthesized Ag NPs against MDR bacteria at different concentrations showed that they revealed a strong dose-

(12.54 \pm 0.57mm, 12.75 \pm 0.78 mm, 12.26 \pm 0.57, 11.58 \pm 0.57mm and 12.53 \pm 0.57 mm. the inhibitory effect of S4, 0.01M AgNO₃ and dried ginger extract is also shown in Table (2) that showed the lower effect of AgNO₃ when compared to AgNPs in S4, besides the non-effect of dried ginger extract.

dependent antimicrobial activity against the tested strains (Table 2). Table (3) also indicates the presence of high significant difference between MIC and MBC for *Klebsiella* spp., *Pseudomonas* spp. and *S. aureus* which had the highest

value for MIC and MBC ($137.5 \pm 68.46 \mu\text{g/ml}$ and $450 \pm 111.80 \mu\text{g/ml}$ respectively).

Mandal *et al.*, (2016) concluded that the MIC and MBC values of AgNPs against bacteria could be used to calculate the tolerance level of each bacterial strain quantitatively so this study used the same method to calculate the tolerance

values of biosynthesized AgNPs against Multi Drug Resistant (MDR) bacteria. The following Equation was used to determine the tolerance level (Tolerance level = MBC/MIC) which is a parameter which reflects the bactericidal capacity of a certain compound by relating both values.

Table (3): Showing MIC, MBC and tolerance value (MBC/MIC) of the biosynthesized Ag NPs for the clinically isolated MDR bacteria; *Klebsiella* spp., *Pseudomonas* spp., *Proteus* spp., *E. coli* and *S. aureus*.

Bacterium	Isolate No.	Concentration ($\mu\text{g/ml}$)		Tolerance value (MBC/MIC)
		MIC	MBC	
<i>Klebsiella</i> spp.	1	062.5	250.0	4
	2	125.0	250.0	2
	3	062.5	125.0	2
	4	062.5	250.0	4
	5	125.0	500.0	4
	6	125.0	500.0	4
	7	250.0	500.0	2
	8	125.0	250.0	2
<i>Pseudomonas</i> spp.	1	062.5	250.0	4
	2	031.25	125.0	4
	3	062.5	250.0	4
	4	125.0	500.0	4
	5	062.5	250.0	4
	6	062.5	250.0	4
	7	125.0	500.0	4
	8	031.25	125.0	4
<i>Proteus</i> spp.	1	125.0	500.0	4
	2	250.0	500.0	2
	3	125.0	500.0	4
	4	062.5	250.0	4
<i>E. coli</i>	1	125.0	500.0	4
	2	250.0	500.0	2
	3	062.5	250.0	4
	4	125.0	500.0	4
	5	062.5	250.0	4
<i>S. aureus</i>	1	250.0	500.0	2
	2	125.0	500.0	4
	3	125.0	500.0	4
	4	062.5	250.0	4
	5	125.0	500.0	4

Table (4): Comparison between Minimum Inhibitory Concentration (MIC) and Minimum Bactericidal Concentration (MBC) of biosynthesized AgNPs to different bacterial isolates

Bacteria	No. of isolates		MIC ($\mu\text{g/ml}$)	MBC ($\mu\text{g/ml}$)	T-test	
					t	p-value
<i>Klebsiella spp.</i>	8	Range	062.50-250.0	125-500	-5.169	0.001**
		Mean \pm SD	117.19 \pm 61.91	328.13 \pm 148.46		
<i>Pseudomonas spp.</i>	8	Range	031.25-125.0	125-500	-5.464	0.001**
		Mean \pm SD	070.30 \pm 36.42	281.25 \pm 145.62		
<i>E.coli</i>	4	Range	062.50-250	250-500	-6.487	0.003*
		Mean \pm SD	125.00 \pm 76.54	400 \pm 136.93		
<i>Proteus spp.</i>	5	Range	062.50-250	250-500	-6.333	0.008*
		Mean \pm SD	140.00 \pm 78.64	437.50 \pm 125		
<i>S. aureus</i>	5	Range	062.50-250	250-500	-7.906	0.001**
		Mean \pm SD	137.50 \pm 68.46	450 \pm 111.80		

Sig.c: significant.

* P \leq 0.05 is significant.

**P \leq 0.001 is highly significant in bold

The effect of biosynthesized AgNPs on MDR bacteria

The influence of AgNPs treatment on the morphology and ultra-structures of bacterial cells were investigated by Scanning Electron Microscope (SEM) and Transmission Electron Microscope (TEM) respectively (Fig.1). SEM micrographs shown that the treated bacterial cells with biosynthesized AgNPs were damaged severely. Many pits and gaps appeared in the micrograph, and their membrane was fragmentary as shown in Fig.1 (b,d). However, smooth and intact bacterial cell wall were obvious are shown in the untreated cells Fig. 1(a,c). TEM micrographs of bacterial cells treated with biosynthesized AgNPs also showed the appearance of big gaps in the cell

membrane, dense particulates inside the cells and partially or completely disintegration with almost destroying of the cells Fig.2(b, d).

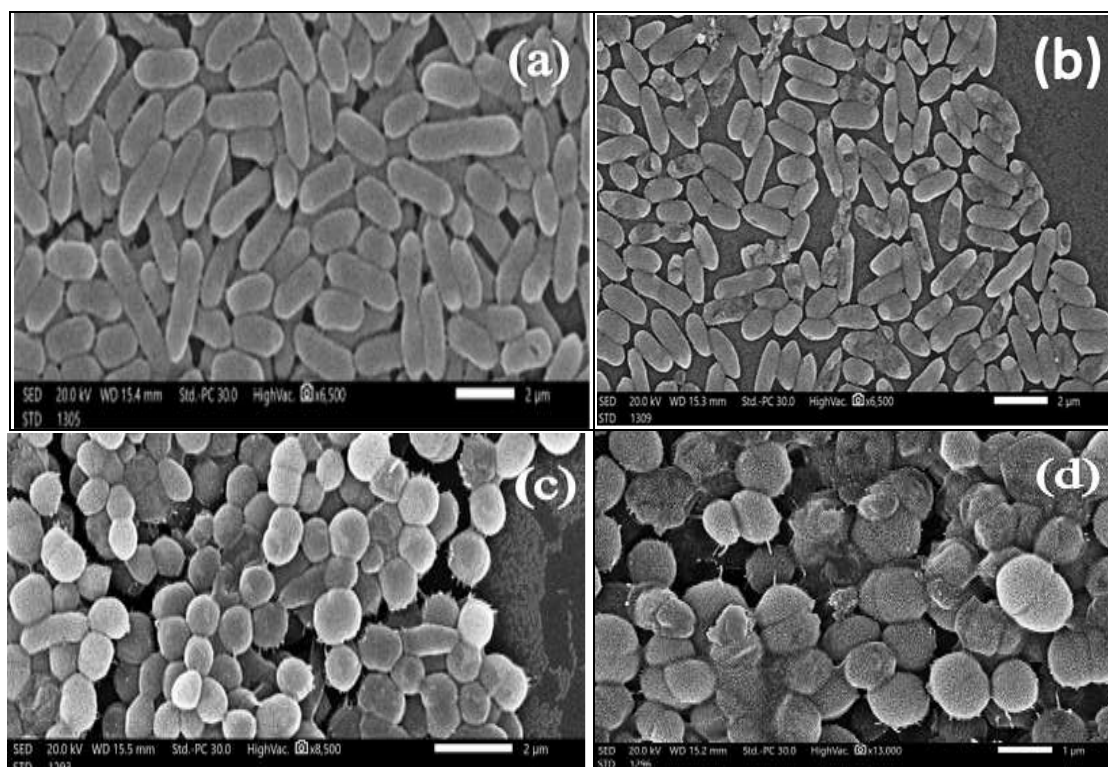


Fig. (1): (a): SEM micrograph of MDR *Proteus* spp. untreated with AgNPs as control. (b): SEM micrograph of MDR *Proteus* spp. treated with AgNPs. (c) SEM micrograph of MDR *S. aureus* untreated with AgNPs as control. (d): SEM micrograph of MDR *S. aureus* treated with AgNPs

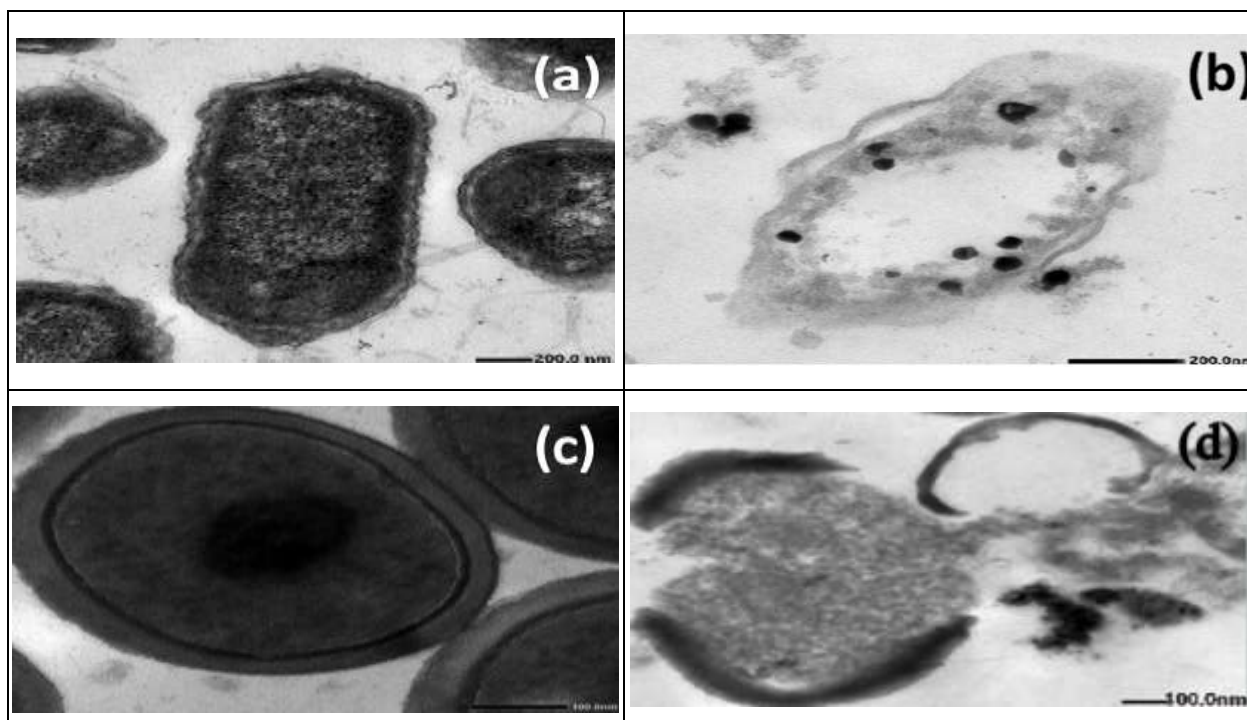


Fig. (2): TEM micrographs of (a): MDR *Proteus* spp. untreated with AgNPs as control. (b): TEM micrographs of MDR *Proteus* spp. treated with AgNPs. (c): TEM micrographs of MDR *S. aureus* untreated with AgNPs as

control. (d): TEM micrographs of MDR *S. aureus* treated with AgNPs

Characterization results of biosynthesized AgNPs

UV-VIS spectroscopy analysis

Solutions color changed from pale yellow to brown, indicating the bio-reduction of silver ions and the creation of silver nanoparticles in the prepared

samples Fig. 3(A,B) The spectra were taken from a wavelength range of 200 to 800 nm which revealed peaks at 431nm for S1 , 424nm for S2 , 457nm for S3 and 452nm for S4. Both of fresh and dried ginger extracts revealed peaks at 280nm (Fig4).

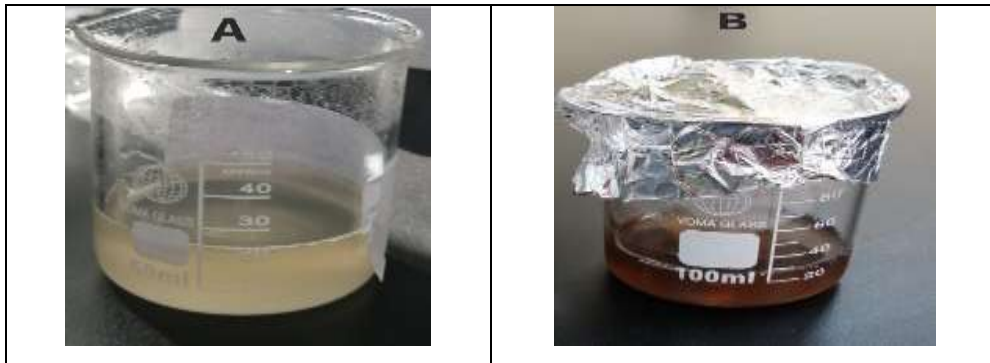


Fig.(3): The Color Changed from pale yellow to brown indicating to formation of silver nanoparticles dried ginger extract + 0.01M Solution of silver nitrate(A) and the biosynthesized AgNPs (B).

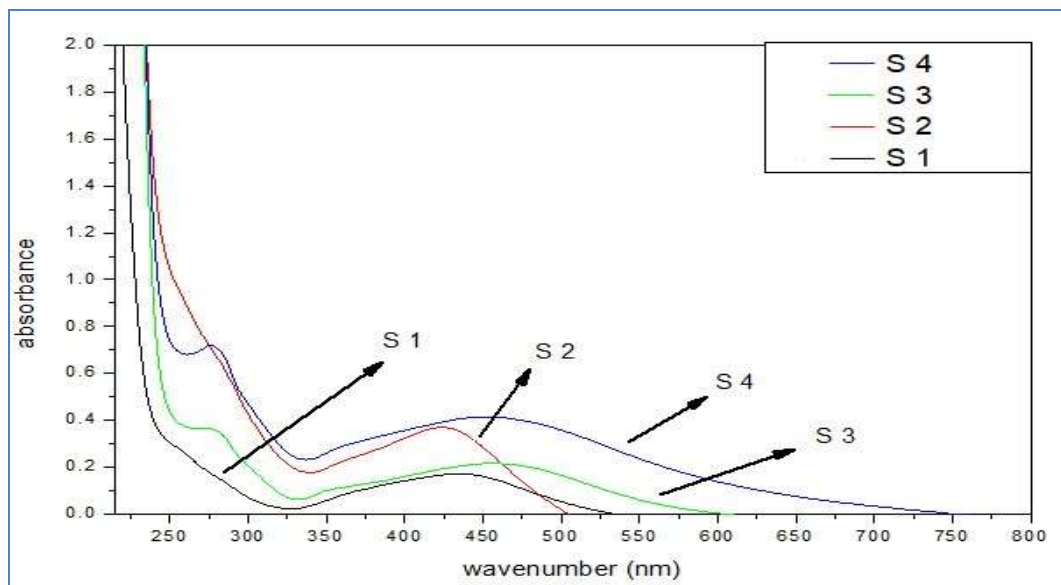


Fig. (4):UV-Vis Spectra of four biosynthesized AgNPs samples where **S1**:the biosynthesized AgNPs by fresh ginger rhizome extract at 30 °C, **S2**: the biosynthesized AgNPs by fresh ginger rhizome extract at 60 °C, **S3**: the biosynthesized AgNPs by dried ginger rhizome extract at 30°C and **S4**: the biosynthesized AgNPs by dried ginger rhizome extract at 60 °C

Zeta potential measurement was used to determine the surface charge of the biosynthesized AgNPs which measured by a zeta analyser (Brookhaven instruments corporation, USA). The results of samples S1, S2, S3 and S4 are -12.98, -13.86, -19.84 and -20.18 mv, respectively as shown in **Fig. 5 (a, b, c, and d)**. Sample 4 (S4) shows the highest had the highest effect on multi drug resistant bacteria and therefore this sample was used for further experimentation. We completed the following characterizations for sample 4 which had the highest effect on multi drug resistant bacteria.

Transmission Electron Micrograph indicates the spherical and irregular shape of AgNPs with diameter range from 3.27 to 23.12 nm (Fig.6).

The X-ray (XRD) pattern of biosynthesized silver nanoparticles produced by *dried Z. officinale* (ginger) extract were obtained using X-ray diffractometer model (GNR APD 2000 Pro) at wavelength 1.54 \AA and is shown in (Fig.7). The diffraction intensities were recorded from 100 to 800 at 2θ angles. The different diffraction peaks were shown at 2θ values of 38.2° , 44.4° , 64.6° and 77.6° corresponding to (111), (200), (220), (311) planes of the diversity of size of silver nanoparticles with crystallinity in nature. These peaks

are matched with the face centered cubic (fcc) structure of silver (JCPDS file No. 04-0783) (**Khan et al., 2012**) with average size 17.9 nm and this result is agreed with the TEM result.

Fourier Transform Infrared Spectroscopy analysis (FTIR)

FTIR measurements help to identify the biomolecules in the dried ginger rhizome extract which responsible for the bio-reduction and the stability to the biosynthesized AgNPs. (Fig.8) shows that the FTIR spectrum of AgNPs is similar to that present in the dried ginger rhizome extract with a slight shift in the band positions. It shows the peaks at 3324 cm^{-1} , 2928 cm^{-1} , 2109 cm^{-1} , 1652 cm^{-1} , 1390 cm^{-1} , 1112 cm^{-1} , 931 cm^{-1} , 859 cm^{-1} , 761 cm^{-1} , and 601 cm^{-1} . The peak at 1652 cm^{-1} is attributed to the stretching vibrations of $\text{C}=\text{C}$ (aliphatic) and the presence of residual NO_3^- is detected by the presence of peak at 1390 cm^{-1} (**Chandan et al., 2011**). The peaks at 1112 cm^{-1} , 931 cm^{-1} , 859 cm^{-1} , 761 cm^{-1} , and 601 cm^{-1} are the strongest indications of heterocyclic compounds presence such as, alkanoids, flavonoids and alkaloids the active components of dried root of *Z.officinale* extract (**Vijaya et al., 2017**).

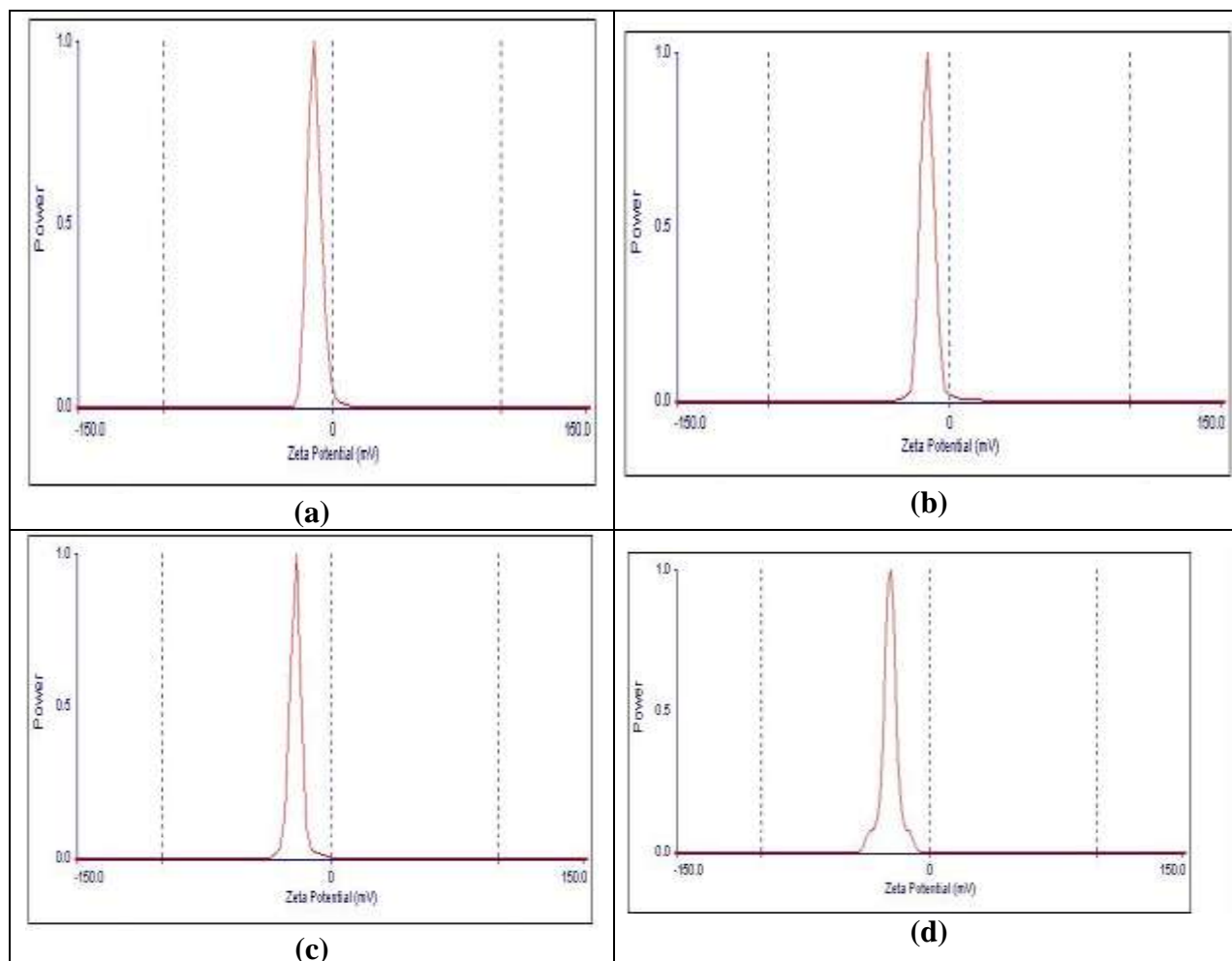


Fig. (5): Zeta potential measurements for biosynthesized AgNPs in S1(a) , S2(b), S3(c) and S4(d)

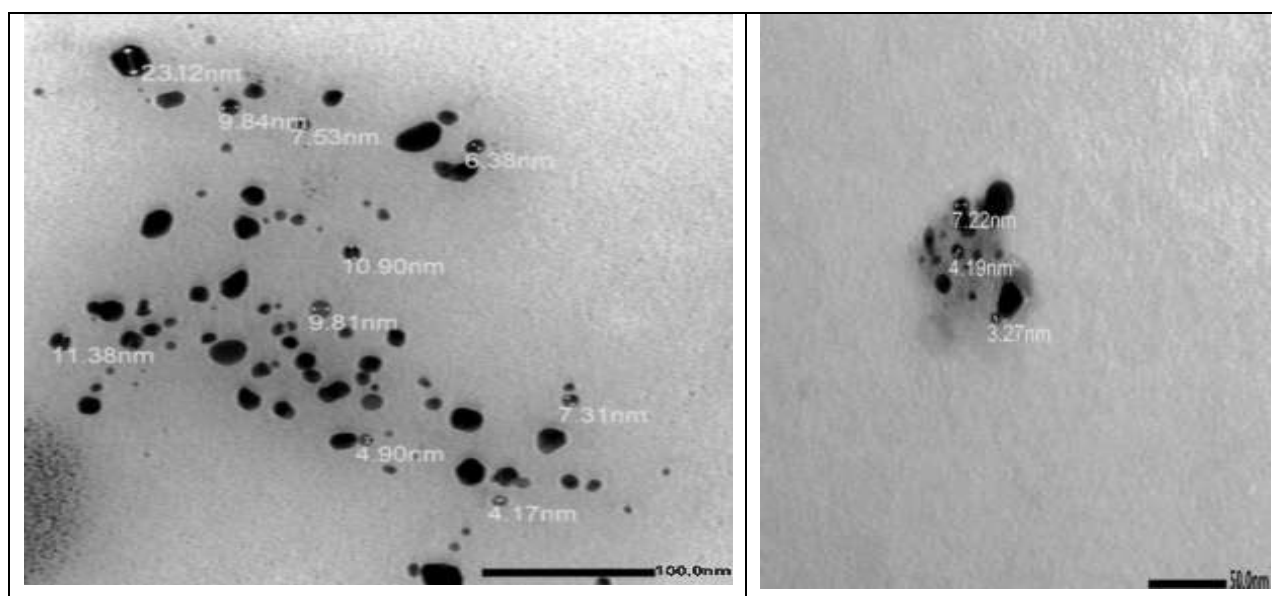


Fig. (6): TEM images shown the biosynthesized AgNPs

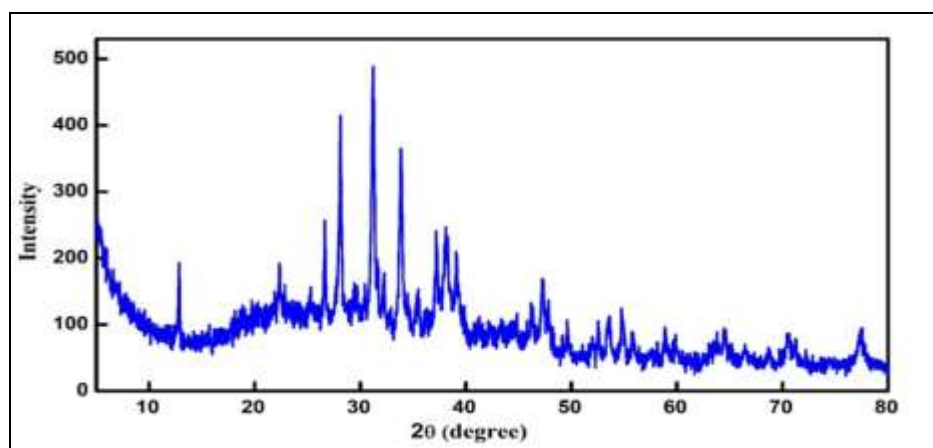


Fig. (7): XRD pattern of biosynthesized AgNPs with dried *Z.Officinale* rhizome extract

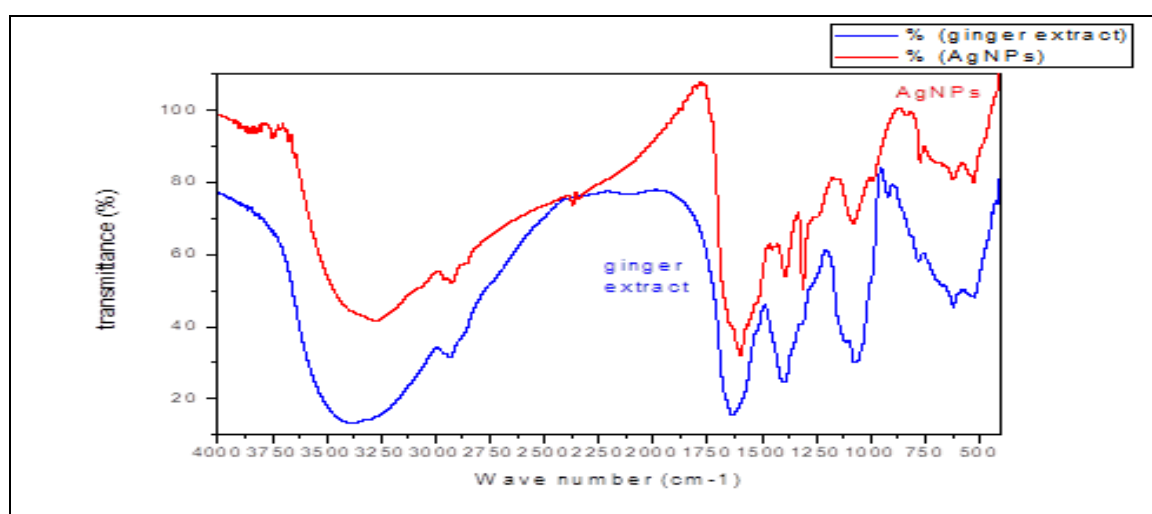


Fig. (8): FTIR spectra of biosynthesized AgNPs in S 4 produced by dried *Z.Officinale* aqueous extract

Discussion

One promising strategy for the environmentally friendly manufacturing of AgNPs is their biological synthesis, which has the dual benefits of being inexpensive and employing bioactive, nontoxic chemicals present in plant extract. (Dipankar *et al.*, 2012). The primary objective of this research is to examine the antimicrobial efficacy of synthesized AgNPs against multidrug-

resistant bacteria by use of fresh and dried ginger extracts (*Z.officinale*).

A grave danger to public health has been the worldwide reporting of multi-drug-resistant bacterial pathogens (Jung *et al.*, 2008). While the control treatment of dried ginger (*Z. Officinale*) extract did not show any zone of inhibition for any of the tested bacterial strains (Vijaya *et al.*, 2017), the antibacterial impact of the silver nitrate solution was lower than that of the biosynthesized AgNPs in

sample 4 (S4). Consistent with other findings, this one shows that biosynthesized AgNPs significantly inhibited the development of MDR bacterial isolates (Vijaya et al., 2017), however, (Li et al., 2017) reported that the silver ions had more potent antibacterial activity than silver nanoparticles, but operating in a manner comparable to the latter. *S.aureus* as gram positive bacteria had the highest MIC and MBC values among all the bacterial species, measuring 137.5 ± 68.46 $\mu\text{g/ml}$ and 450 ± 111.80 $\mu\text{g/ml}$, respectively. The results indicate that the growth inhibition was caused by the penetration of AgNPs into the bacterial cell. This helps to explain why Gram positive and Gram negative bacteria have different cell wall compositions (Thiel et al., 2007). It is well known that Gram-negative bacteria had an outer membrane outside the peptidoglycan layer that was lacking in Gram-positive organisms. The main role of the outer membrane is acting as a selective permeability barrier that help gram negative bacteria to be protected from hurtful agents, such as toxins, drugs, detergents and analytic enzymes and also penetrating nutrients to maintain the bacterial growth. The lipid bilayer of outer membrane is asymmetric: the inner part mostly contains closely-packed phospholipid

chains, while the outer part is composed of the lipopolysaccharide (LPS) molecules as reported by (Amro et al., 2000). Pal et al., (2007) mentioned that the lipopolysaccharides presence in Gram-negative cell wall enhance AgNPs adhesion to it and affecting cell wall permeability and cell integrity. Mussin et al., (2021) reported that the MBC/MIC ratio can determine if the bacteria are susceptible, tolerant, or resistant to a certain agent that is being challenged. A compound was considered bactericidal or fungicidal agent if the ratio (MBC/MIC) was ≤ 4 , and bacteriostatic if the ratio was > 4 . The tolerance levels of bacterial isolates revealed that the biosynthesized AgNPs had a bactericidal effect on the bacterial isolates being investigated. We still don't fully understand how biosynthesized AgNPs penetrate bacteria. The morphological alterations in membranes treated with AgNPs have been documented in earlier research. Because of these alterations, membrane permeability increased dramatically, rendering bacterial cells incapable of controlling transport across the plasma membrane and ultimately leading to cell death (Ivask et al., 2009). By interacting with biological macromolecules like DNA and controlling enzymes, AgNPs have clearly caused harm after penetrating the bacterial cell (Morones et al., 2005).

The proposed mechanism of action for AgNPs involves the penetration of the outer membrane then the subsequent leaking of cellular components. When silver nanoparticles (AgNPs) penetrate a cell's inner membrane, they release reactive oxygen species (ROS), which can stunt the cell's proliferation. In the end, cells decompose and die (**Li et al., 2010**). **Su et al., (2009)** reported that the antimicrobial activity of the AgNPs including the generation of intracellular ROS and the rising of intracellular ROS levels is the main essential mediators for death of the cell. The production of ROS could be caused by the impeded electronic transport along the respiratory chain in the damaged plasma membrane causing disturbance in the cell activity gradually until the cell death.

A two-hour color shift from light yellow to brown was observed after adding aqueous extracts of *Z. officinale* rhizome to a silver nitrate solution (0.01M), indicating the synthesis of AgNPs in the solution. A distinctive peak at 458 nm was shown in UV-Vis spectra at wavelengths ranging from 200 to 800 nm, which supported this claim (**Mulvaney, 1996**). A single surface plasmon resonance band was seen in the absorption spectra of AgNPs produced in a prior research, suggesting the presence of AgNPs with a spherical form (**Iravani et al., 2014**). It was observed at different

temperatures (30 °C and 60 °C) to verify that temperature affects the synthesis of AgNPs. Prior research by indicated that the production of AgNP rose in tandem with rising temperature (**Liu et al., 2017**).

Zeta potential of biosynthesized AgNPs using *Z.officinale* aqueous extracts is shown in **Fig.(5)**, this means that the most stable nano-colloidal solution is the one with the most negative charge, as described by (**Ibrahim et al., 2016**). In agree with (**Dinda et al. 2019**), TEM micrographs showed that silver nanoparticles with both round and non-round shapes were present with a diameter range from 3.27 nm to 23.12 nm. Antibacterial activity is enhanced by the spherical form of AgNPs compared to rod and wire shapes of the same diameter. This suggests that the antibacterial impact of shape is a result of the specific and wide surface area as well as facet reactivity (**Raza et al., 2016**). Dried *Z.officinale* (ginger) extract biosynthesized AgNPs at 60°C (S4) show an X-ray (XRD) pattern with various diffraction patterns matching to planes of size variety of silver nanoparticles with crystallinity. The face-centered cubic (fcc) structure of silver is matched with these peaks. (**khan et al., 2012**) on average 17.9 nm in size, which is in agreement with the

TEM finding. Other, less clearly defined peaks may have emerged as a result of organic contaminants introduced by the plant extract. Moreover, comparable peaks have been described in earlier research that used herbal extract to produce AgNPs (**Taghavizadeh Yazdi et al., 2018; Hamidi et al., 2019**). The phytochemical components in *Z. officinale* (ginger) water extracts that were shown to reduce and cap AgNO₃ were described by (**Vijaya et al. 2017**) on the job of stabilizing AgNPs in the colloidal solution and carrying out their environmentally friendly synthesis. By analyzing the bio-reduction and stability of the dried ginger rhizome extract to the produced AgNPs, FTIR measurements help identify the biomolecules responsible for these processes. Dried ginger rhizome extract contains a number of heterocyclic compounds, which are water-soluble, and it is these compounds that formed functional groups, which stabilized the size of AgNPs and were responsible for capping them. Alkanoids, flavonoids, and other phytochemicals have been shown to function as capping ligands in the production of Ag-NPs (**Chandan et al., 2011**). Phytochemical components in ginger extracts were reportedly used in the biosynthesis of AgNP by means of C=O, C=C, and C-O groups. The small shifting of the band locations indicates

that the -OH group is oxidized to C=O, which is responsible for the biosynthesis of AgNPs. The extract's alkaloids, flavonoids, starch, and alkanoids are responsible for the decrease and stability of AgNPs (**Sreeram et al., 2008**). Prior research on AgNPs produced environmentally also found comparable FTIR patterns (**Otunola et al., 2017**).

References

- Amro, N. A., Kotra, L. P., Wadu-Mesthrige, K., Bulychev, A., Mobashery, S., Liu, G., (2000)** High-resolution atomic force microscopy studies of the *Escherichia coli* outer membrane: structural basis for permeability. *Langmuir*, 16: 2789–2796
- Ansari S., Jha R. K., Mishra S. K., Tiwari B. R., Asaad A. M., (2019)**. Recent advances in *Staphylococcus aureus* infection: Focus on vaccine development. *Infect. Drug Resist.*, 12:1243–1255.
- Begum N. A., Mondal S., Basu S., Laskar R. A., Mandal D., (2009)**. Biogenic synthesis of Au and Ag nanoparticles using aqueous solutions of Black Tea leaf extracts, *Colloids Surf. B.*, 71(1):113-118.
- Bar H., Bhui D. K., Sahoo G. P., Sarkar P., Bes P., Misra A., (2009)**. Green synthesis of silver nanoparticles using seed extract of *Jatropha curcas*, *Colloids Surf. A Physicochem. Eng. Asp.*, 348: 212-216.
- Bauer A. W., Kirby W. M., Sherris J. C. and Turck M., (1966)**. Standardized Antibiotic susceptibility testing by a single disk method, *Am. J. Clin. Pathol.*, 45(4):493-6.

- Chandan S., Vineet S., Naik Pradeep K. R., Vikas K., Harvinder S., (2011).** Role of Biogenic Synthesis of Biocompatible Nano Gold Particles and Their Potential Applications - A Review, *Digest J. Nanomater. Biostruct.* 6:535-542.
- Cheesbrough.M., (2006).** District laboratory practice in tropical countries, *C.U.P.* 2: 62-127.
- Chethana G. S., Hari venkatesh K. R., Mirzaei F., and Gopinath S. M., (2013).** Review on multidrug resistant bacteria and its implication in medical sciences, *J. Biol. Sci. Opin.*, 1(1): 32–37.
- Clinical and Laboratory Standards Institute, CLSI (2012).** Methods for Dilution Antimicrobial Susceptibility Tests for Bacteria That Grow Aerobically; Approved. Standard ,9th ed., M07-A9 , 32 (2).
- Clinical Laboratory and Standard Institute. CLSI (2021).** Performance standards for antimicrobial susceptibility testing. (30th ed). M100. Wayne, PA.
- Dinda G., Halder D., and Mitra A., (2019).** Phytosynthesis of silver nanoparticles using *Zingiber officinale* extract: evaluation of their catalytic and antibacterial activities, *J. Disper. Sci. Technol.*, 41(14):1-8.
- Dipankar C., and Murugan S., (2012).** The green synthesis, characterization and evaluation of the biological activities of silver nanoparticles synthesized from *Iresine herbstii* leaf aqueous extracts, *Colloids surf B Biointerfaces*, 98:112-9.
- Elechiguerra J. L., Burt J. L., Morones J. R., Bragado A.C., Gao X., Lara H. H., and Yacaman M. J., (2005).** Interaction of silver nanoparticles with HIV-1, *J. Nanobiotechnol.*, 3:1–10.
- El-Refai A. A., Ghoniem G. A., El-Khateeb A.Y., and Hassaan M. M., (2018).** Eco-friendly synthesis of metal nanoparticles using ginger and garlic extracts as biocompatible novel antioxidant and antimicrobial agents. *J. Nanostructure Chem.*, 8:71-81.
- El-Shennawy G., Abd Ellatif R., Badran S., and El-Sokkary R., (2020).** Silver nanoparticles: A potential antibacterial and antibiofilm agent against biofilm forming multidrug resistant bacteria. *M.I.D.*, 1(2):77-85.
- Erjaee H., Rajaian H., Nazifi S., (2017).** Synthesis and characterization of novel silver nanoparticles using *Chamaemelum nobile* extract for antibacterial application. *Adv. Nat. Sci: Nanosci. Nanotechnol.*, 8(2): 025004.
- Hamidi A., Taghavizadeh Yazdi M. E., Amiri M. S., Hosseini H. A., and Darroudi M., (2019).** Biological synthesis of silver nanoparticles in *Tribulus terrestris* L. extract and evaluation of their photocatalyst, antibacterial, and cytotoxicity effects. *Res. Chem. Intermediates*, 45:2915-2925.
- He X., Li S., and Kaminskyj S. G., (2013).** Using *Aspergillus nidulans* to identify antifungal drug resistance mutations, *Eukaryot. Cell*, 13 (2):288–294.
- Holt J. G., Krieg N. R., Sneath P. H. A., Staley J. T., and Williams S. T., (1994).** *Bergey's Manual of Determinative Bacteriology.* (9th ed), Williams and Wilkins Baltimore, MD 1–787.
- Hu D., Gao T., Kong X., Ma N., Fu J., Meng L., and Latif S., (2022).** Ginger (*Zingiber officinale*) extract mediated green synthesis of silver nanoparticles and evaluation of their antioxidant activity and potential catalytic reduction activities with Direct Blue 15 or Direct Orange 26. *Plos One* 17(8):e0271408.
- Hwang E.T., Lee J H., Chae Y J., Kim, Y S., Kim, B C., Sang, B I., Gu M. B.,**

- (2008) Analysis of the toxic mode of action of silver nanoparticles using stress-specific bioluminescent bacteria. *Small*, 4, 746–750.
- Ibrahim I. M., Abbas A.K., and Naser D.K., (2016).** Synthesis and zeta potential of noble metals (Pt, Au, Ag AND Cu) nanoparticles prepared by pulse laser ablation, *sci.int.(lahore)*, 28(5):4371-4375.
- Iravani S., Korbekandi H., Mirmohammadi S. V., and Zolfaghari B., (2014).** Synthesis of silver nanoparticles: Chemical, physical and biological methods. *Res. Pharm. Sci.*, 9: 385–406.
- Ivask A., Rõlova T., and Kahru A., (2009).** A suite of recombinant luminescent bacterial strains for the quantification of bioavailable heavy metals and toxicity testing. *BMC Biotechnology*; 9(1): 41.
- Jain J., Arora S., Rajwade J M., Omray P., Khandelwal S., and Paknikar K. M., (2009)** Silver nanoparticles in therapeutics: development of an antimicrobial gel formulation for topical use. *Mol. Pharm.*, 6, 1388–1401.
- Jung W. K., Koo H. C., Kim K.W., Shin S., Kim S. H., and Park Y. H., (2008).** Antibacterial Activity and Mechanism of Action of the Silver Ion in *Staphylococcus aureus* and *Escherichia coli*. *Appl. Environ. Microbiol.*, 74, 2171–2178.
- Khalil M. A., El Maghraby G. M., Sonbol F. I., Allam N. G., Ateya P. S. and Ali S. S., (2021)** Enhanced Efficacy of Some Antibiotics in Presence of Silver Nanoparticles Against Multidrug Resistant *Pseudomonas aeruginosa* Recovered From Burn Wound Infections. *Front. Microbiol.*, 12:648560.
- Khan M. M., Kalathil S., Lee J., and Cho M.H., (2012).** Synthesis of cysteine capped silver nanoparticles by electrochemically active biofilm and their antibacterial activities. *Bull. Korean Chem Soc.*, 33(8):2592–2596.
- Ki V. and Rotstein C., (2008)** Bacterial Skin and Soft Tissue Infections in Adults: A Review of Their Epidemiology, Pathogenesis, Diagnosis, Treatment and Site of Care. *Can. J. Infect. Dis. Med. Microbiol.*, 19:173–184.
- Klevens R. M., Morrison M. A., Nadle J., Petit S., Gershman K., Ray S., Harrison L.H., Lynfield R., Dumyati G. and Townes J. M., Craig A. S., Zell E. R., Fosheim G. E., McDougal L. K., Carey R. B., and Fridkin S. K., (2007).** Invasive methicillin-resistant *Staphylococcus aureus* infections in the United States. *J.A.M.A.*, 298:1763–71.
- Kouvaris P., Delimitis A., Zaspalis V., Papadopoulos D., Tsipas S.A., and Michailidis N., (2012).** Green synthesis and characterization of silver nanoparticles produced using *Arbutus Unedo* leaf extract. *Materials Lett.*, 76:18-20.
- Krishnaraj C., Jagan E.G., Rajasekar S., Selvakumar P., Kalaichelvan P. T., and Mohan N., (2010).** Synthesis of silver nanoparticles using *Acalypha indica* leaf extracts and its antibacterial activity against water borne pathogens, *Colloids Surf. B. Biointerfaces*, 76:50–6.
- Li W. R., Xie X. B., Shi Q. S., Zeng H. Y., OU-Yang Y.S., and Chen Y. B., (2010).** Antibacterial activity and mechanism of silver nanoparticles on *Escherichia coli*. *Appl. Microbiol. Biotechnol.*, 85: 1115– 1122.
- Li W. R., Sun T. L., Zhou S. L., Ma Y. K., Shi Q.S., Xie X.B., and Huang X.M., (2017).** A comparative analysis of antibacterial activity, dynamics and

- effects of silver ions and silver nanoparticles against four bacterial strains. *Int. Biodeterior. Biodegrad.*, 123: 304–310
- Liu H., Zhang H., Wang J., and Wei J., (2017).** Effect of temperature on the size of biosynthesized silver nanoparticle: Deep insight into microscopic kinetics analysis. *Arab. J. Chem.*, 13: 1011–1019.
- Mandal D., Dash S. K., Das B, Chattopadhyay S., Ghosh T., Das D., Roy S., (2016)** Bio-fabricated silver nanoparticles preferentially targets Gram positive depending on cell surface charge. *Biomed. Pharmacother.*, 83 :548-558.
- Morones J.R., Elechiguerra J. L., Camacho A., and Ramirez J. T., (2005).** The bactericidal effect of silver nanoparticles. *J. Nanotechnol.* 16: 2346–2353.
- Mulvaney P., (1996).** Surface plasmon spectroscopy of nanosized metal particles. *Langmuir*; 12:788–800.
- Mussin J, Robles-Botero V., Casañas-Pimentel R., Rojas F., Angiolella L., San Martín-Martínez E. and Giusiano G., (2021)** Antimicrobial and cytotoxic activity of green synthesis silver nanoparticles targeting skin and soft tissue infectious agents. *Sci. Rep.*, 11:14566.
- Nosanchuk J. D., Lin J., Hunter R. P., and Aminov R. I., (2014).** Low-dose antibiotics: current status and outlook for the future. *Front. Microbiol.*, 5:478.
- Otunola G. A., Afolayan A. J., Ajayi E. O., and Odeyemi S. W., (2017).** Characterization, antibacterial and antioxidant properties of silver nanoparticles synthesized from aqueous extracts of *Allium sativum*, *Zingiber officinale*, and *Capsicum frutescens*. *Pharmacogn. Mag.*, 13(5):201.
- Pal S., Tak Y.K., Song J. M., (2007).** Does the antibacterial activity of silver nanoparticles depend on the shape of the nanoparticle? A study of the gram negative bacterium *Escherichia coli*. *Appl. Environ. Microbiol.*, 27: 1712– 1720.
- Priyaa H. G., and Kumudini B. S., (2014).** Biological Synthesis of Silver Nanoparticles using Ginger (*Zingiber Officinale*) Extract, *J. Environ Nanotechnol.*, 3:32-40.
- Raafat M., El-Sayed A. S. A., and El-Sayed M.T., (2021).** Biosynthesis and Anti-Mycotoxigenic Activity of *Zingiber officinale* Roscoe-Derived Metal Nanoparticles. *Molecules*, 26:2290.
- Rai M., Deshmukh S. D., Ingle A. P., Gupta I. R., Galdiero M., and Galdiero S., (2014).** Metal nanoparticles: The protective nanoshield against virus infection, *Crit. Rev Microbiol.*, 42:46-56.
- Rasool N., Saeed Z., Pervaiz M., Ali F., Younas U., Bashir R., Bukhari S.M., Khan R.R.M., Jelani S., and Sikandar R., (2022).** Evaluation of essential oil extracted from ginger, cinnamon and lemon for therapeutic and biological activities. *Biocatal. Agric. Biotechnol.*, 44:102470.
- Raza M. A., Kanwal Z., Rauf A., Sabri A.N., Riaz S., and Naseem S., (2016).** Size-and shape-dependent antibacterial studies of silver nanoparticles synthesized by wet chemical routes. *J. Nanomater.*, 6:74.
- Şahin M., and Gubbuk I. H., (2019).** Green synthesis of antioxidant silver and platinum nanoparticles using ginger and turmeric extracts and investigation of their catalytic activity. *J.O.T.C.S.A.*, 6(3):403-410.
- Salomoni R., Léo, P., Montemor, A F., Rinaldi B G and Rodrigues M.(2017)**

Antibacterial effect of silver nanoparticles in *Pseudomonas aeruginosa*. *Nanotechnol. Sci. Appl.* 10: 115–121.

Singh R.P., Magesh S., Rakkiyappan C. (2011) GINGER (*ZINGIBER OFFICINALE*) ROOT EXTRACT: A SOURCE OF SILVER NANOPARTICLES AND THEIR APPLICATION *I.J.B.E.S.T.*, 2(3).

Solomon D. S., Mozghan B., Jeyarajasingam V. A., Rutkowsky A. S., (2007). Synthesis and Study of Silver Nanoparticles, *J.Chem.Edu.*, 84 (2):322.

Sondi I. and Sondi S. B., (2004).

Silver nanoparticles as antimicrobial agent: a case study on *E. coli* as a model for Gram-negative bacteria *J. Interface Sci.*, 275: 177.

Song J. Y., Kim B. S., (2009). Rapid biological synthesis of silver nanoparticles using plant leaf extracts, *Bioprocess Biosys. Eng.*, 32:79.

Sreeram K.J., Nidhin M., Nair B. U., (2008). Microwave assisted template synthesis of silver nanoparticles, *Bull. Mater. Sci.*31:937-942.

Su H., Chou C., Hung D., Lin S., Pao I., Lin J., Huang F. L., Dong R. X., Lin J. J. (2009). The disruption of bacterial membrane integrity through ROS generation induced by nanohybrids of silver and clay. *Biomater*, 30: 5979–5987.

Taghavizadeh Yazdi M. E., Khara J., Sadeghnia H.R.(2018). Biosynthesis, characterization, and antibacterial activity of silver nanoparticles using *Rheum turkestanicum* shoots extract, *Res. Chem. Intermed.*, 44(2):1325–1334.

Tahmasebi P., Javadpour F., Sahimi M., (2015). Transport in Porous Media.*Sci.Rep.*, 110 (3): 521–531.

Thiel J., Pakstis L., Buzby S., Raffi M., Ni C., Pochan D.J., Ismat Shah S., (2007). Antibacterial Properties of Silver-Doped Titania, *Small*, 3(5): 799 – 803.

Vijayaa Judith J., Jayaprakasha N., Kombaiaha K., Kaviyarasuc K., John Kennedy L., Jothi Ramalingamf R., Al-Lohedanf Hamad A., Mansoor-Ali V.M., and Maaza M., (2017). Bioreduction potentials of dried root of *Zingiber officinale* for a simple green synthesis of silver nanoparticles: Antibacterial studies, *J. Photochem. Photobiol. B. Biol.*, 177:62–8.

Walker B., Barrett S., Polasky S., Galaz V., Folke C., Engstrom G., Ackerman F., Arrow K., Carpenter S., Chopra K., Daily G., Ehrlich P., Hughes T., Kautsky N., Levin S., Mäler K.G., Shogren J., Vincent J., Xepapadeas T., and de Zeeuw A., (2009). Environment. Looming global-scale failures and missing institutions, *Sci.*,325: 1345–6.

Yang H., Ren Y., Wang T., Wang C. (2016). Preparation and antibacterial activities of $Ag/Ag^+/Ag^{3+}$ nanoparticles composites made by pomegranaten (*punica granatum*) rind extract. *Results Phys.*, 6: 299-304.

Yue B., Yang J., Wang Y., Huang C.Y., Dave, R., and Pfeiffer R. (2004). Particle encapsulation with polymers via in situ polymerization in supercritical CO_2 . *Powder Technol.*, 146(2):32-45.

النشاط المضاد للبكتيريا لجسيمات الفضة النانوية التي تم تخليقها حيويًا بواسطة الزنجبيل على البكتيريا المقاومة للأدوية المتعددة

محمد مدحت غريب^١ ، ماجد عبد التواب القمري^٢ ، عزه محمود حسن^٣ ، سالي محمد نجيب جمعة^١

^١ قسم النبات و الميكروبيولوجي - كلية العلوم - جامعة المنوفية.

^٢ معهد علوم و تكنولوجيا النانو - جامعة كفر الشيخ.

^٣ قسم الميكروبيولوجيا الطبية و المناعة - كلية الطب - جامعة طنطا.

يعتبر التخليق الحيوي لجسيمات الفضة النانوية باستخدام مستخلص الزنجبيل إحدى الطرق الصديقة للبيئة ورخيصة التكلفة. قد تم تمييز جسيمات الفضة النانوية المنتجة باستخدام التحليل الطيفي للأشعة المرئية وفوق البنفسجية وحيود الأشعة السينية والتحليل الطيفي للأشعة تحت الحمراء وتحليل جهد زيتا والمجهر الإلكتروني النافذ الذي أوضح بأن لها أشكال كروية وغير منتظمة يتراوح قطرها من ٣.٢٧ نانومتر إلى ٢٣.١٢ نانومتر كما أظهرت هذه الجسيمات نشاطًا قويًا مضادًا للميكروبات ضد البكتيريا المعزولة سريريًا والمقاومة للأدوية المتعددة وهي المكورات العنقودية الذهبية والإشريكية القولونية و *S. aureus* و *E. coli* و *K. pneumoniae* و *P. aeruginosa*. وقد تم إجراء الأختبارات البيوكيميائية والحساسية للمضادات الحيوية في قسم الأحياء الدقيقة الطبية والمناعة، كلية الطب، جامعة طنطا. ثم درس تأثير جسيمات الفضة النانوية المخلفة حيويًا على البكتيريا المقاومة للأدوية المتعددة المعزولة سريريًا بطريقة انتشار القرص (Disk diffusion method) بالإضافة إلى تقدير الحد الأدنى للتركيز المثبط والحد الأدنى لتركيز مبي تراوحت التقديرات بين ٢٥، ٣١ ميكروغرام/مل إلى ٢٥٠ ميكروغرام/مل ومن ١٢٥ ميكروغرام/مل إلى ٥٠٠ ميكروغرام/مل، على التوالي من سلالات البكتيريا المضادة للأدوية المتعددة المختبرة. وقد تم رؤية بعض الخلايا البكتيرية (المكورات العنقودية الذهبية والبروتيتوس) قبل وبعد التأثير بهذه الجسيمات حيث أظهر تمزق غشاء الخلية مما أدى إلى موت الخلايا مقارنة بالخلايا البكتيرية غير المعالجة التي تم الكشف عنها بواسطة التصوير بالمجهر الإلكتروني النافذ والمجهر الإلكتروني الماسح.